 FDMP, vol.7, no.4, pp.341-355, 2011

Flow-Induced Forces in Agglomerates

J.J. Derksen[1] **and D. Eskin**[2]

Abstract: Direct simulations of laminar solid-liquid flow in micro-channels with full resolution of the solid-liquid interfaces have been performed. The solids phase consists of simple agglomerates, assembled of monosized, spherical particles. The flow of the interstitial liquid is solved with the lattice-Boltzmann method. Solids and fluid dynamics are two-way coupled. The simulations keep track of the flow-induced forces in the agglomerates. The effects of agglomerate type (doublets, triplets, and quadruplets), solids loading, and channel geometry on (the statistics of the) flow and collision-induced forces have been investigated. By comparing these forces with agglomerate strength, we would be able to assess the potential of micro-channels as agglomerate breakage devices.

Keywords: Agglomerates, direct simulations, lattice-Boltzmann, suspensions.

1 Introduction

In many processes involving solid particle formation or solids handling, particles have a tendency to stick together. In crystallization processes crystals tend to agglomerate due to the supersaturated environment they are in. Suspension polymerization processes go through a "sticky-phase" with significant agglomeration levels. In colloidal systems a variety of interactions can cause agglomeration (related to Van der Waals forces, electrolyte-induced interactions, surface chemistry), and stabilization of colloids is a central issue. In bio-related applications agglomeration plays a role in such diverse fields as blood flow and bio-molecular cross-linking of particles. The application which is driving the present research is the behavior of asphaltenes, more specifically their deposition on rock walls in oil reservoirs [Boek, Ladva, Crawshaw, and Padding (2008), and references therein]. Asphaltene agglomeration is a key step in asphaltene deposition since the agglomerate size and the agglomerate sticking probability to the wall are intimately related: only relatively small agglomerates stick to the wall while bigger ones are removed with the

[1] Chemical & Materials Engineering, University of Alberta, Edmonton, Alberta, Canada
[2] Schlumberger DBR Technology Center, Edmonton, Alberta, Canada

flow. The agglomerate size distribution evolves as a result of agglomeration and also de-agglomeration (i.e. breakage of agglomerates).

For an agglomeration event to occur, particles (primary particles and/or agglomerates) need to collide first. Typically collisions are induced by Brownian motion, gravity, and velocity gradients in the fluid carrying the particles since these phenomena bring about relative velocities between particles. Also particle inertia can be a source of collisions.

Next to promoting collisions, fluid velocity gradients and particle-particle interactions are potential reasons for agglomerate breakage since they cause mechanical loads on agglomerates. In this paper we focus on the latter aspect: We investigate the mechanical load on agglomerates due to deformation of the surrounding liquid and the presence of other particles/agglomerates. Interactions with other particles/agglomerates can be either direct (collisions) or indirect, e.g. transmitted by the interstitial liquid.

In modeling processes involving agglomeration, population balances are often used to keep track of agglomerate size distributions (ASD's) [Hounslow and Reynolds (2006), Aamir, Nagy, Rielly, Kleinert, and Judat (2009)]. In order to equip population balances with adequate agglomeration and breakage physics, rate laws (usually termed kernel functions) are being developed that relate numbers of agglomeration and breakage events per unit volume and time to local (flow and agglomerate) conditions. With the purpose of devising kernels, there is extensive literature on agglomeration and breakage as a result of hydrodynamics for small (though non-Brownian) agglomerates in turbulent flow [see Bäbler, Morbidelli, and Baldyga (2008) and references therein]. Small in this context means that the agglomerate size is significantly smaller than the smallest dynamical scale of turbulence, i.e. the Kolmogorov scale. If this is the case the flow field surrounding the agglomerate can be assumed to scale with the (local) rate of energy dissipation and be of some canonical, simple nature, and disruptive forces, as well as collision probabilities can be modeled fairly accurately based on Stokes flow principles [see e.g. Nir and Acrivos (1973); Bäbler, Morbidelli, and Baldyga (2008)]. In a previous paper [Derksen (2008)], however, it was argued that the situation significantly complicates if the agglomerate (in that paper a doublet of spheres) has a size of the same order as the Kolmogorov scale, or is larger. It then experiences an inhomogeneous flow and the (fluctuating) details of the hydrodynamics around it are crucial for its internal forces and thus breakage probability. A similar situation occurs in micro-reactor equipment where (as an example) agglomerate slurries are being sent through nozzle-shaped micro-channels to facilitate breakage [Zaccone, Soos, Lattuada, Wu, Bäbler, and Morbidelli (2009)]. Again there is a non-trivial flow field around the agglomerate that induces internal forces that can break it.

From the above it may be clear that information regarding flow-induced and particle-interaction-induced forces in agglomerates are key in describing their probability to break. In this paper a computational procedure is presented to determine these forces from first principles. In the computations, agglomerates are assembled of primary spherical particles all having the same size, and released in a flow field. We directly solve the flow around the agglomerates, and fully couple flow and agglomerate motion. The force and torque required to keep a primary particle attached to the agglomerate follow from this computational procedure. Comparing that force and/or torque with a measure of the agglomerate strength allows for assessing the breakage probability. Usually a primary sphere has more than one contact point with the other primary spheres in the agglomerate. This (in general) makes it impossible to calculate the force and torque at each contact point from the momentum balance directly. However, for a few simple agglomerate configurations the force and torque per contact point can be determined with minimal assumptions.

It should be noted that during the simulations presented in this paper the agglomerates keep their integrity; we do not actually break them. The results of the simulations comprise detailed representations (time series, probability density functions) of the flow-induced forces and torques in agglomerates as a function of process conditions. From this detailed information breakage probability can be assessed once data regarding the mechanical strength of the specific agglomerates at hand is available.

In this paper we first define the flow systems in terms of their dimensionless parameters, and indicate which part of the parameter space we will be exploring. Then the computational framework for calculating the flow-induced forces in agglomerates is explained. We then apply the method to flow of agglomerate slurries in micro-channels where we compare forces in different types of simple agglomerates, viz. doublets, triplets arranged in triangles, and quadruplets arranged in tetrahedrons, all made of equally sized spherical particles. By considering a range of solids volume fractions of the agglomerate slurries, the role of particle-particle interactions on the mechanical load on agglomerates is assessed. Furthermore, a few different micro-channel layouts have been compared. Specifically we compare straight, square channels with channels having contractions.

2 Flow system & parameter space

The basic flow geometry in this study is a square channel; see Fig. 1 for a definition of its dimensions and coordinate system. The laminar flow in the channel is driven by a body force f_0 acting in the x (=streamwise) direction mimicking a pressure gradient (or, if vertically placed, gravity). At the four side walls a no-slip boundary condition applies; the system is periodic in streamwise direction. A Reynolds num-

ber characterizing the flow in the channel can be based on the wall shear velocity $u_\tau = \sqrt{\frac{\tau_w}{\rho}}$: $Re_w = \frac{u_\tau H}{\nu}$ with ν the kinematic viscosity of the liquid in the channel, and ρ its density. The average wall shear stress τ_w follows from an overall force balance: $4H\tau_w = H^2 f_0$ so that eventually $Re_w = \frac{1}{2}\frac{H^{3/2} f_0^{1/2}}{\rho^{1/2}\nu}$.

Inspired by work due to Zaccone, Soos, Lattuada, Wu, Bäbler, and Morbidelli (2009), in some of the simulations the channel has a contraction as defined in the bottom panels of Fig. 1. The contraction is two-dimensional, i.e. the channel is only contracted locally in the z-direction; the width in the y-direction remains H. The Reynolds number definition for the contracted channel cases is the same as for the uniform channel. All channels considered have length-over-width aspect ratio $\frac{L}{H} = 2.0$.

In the liquid that fills the channel agglomerates are released. They consist of equally sized spheres with radius a. Three types of agglomerates will be considered: (1) two touching spheres forming a doublet; (2) three touching spheres (triplet) forming a triangle (two contact points per primary sphere); (3) four touching spheres (quadruplet) forming a tetrahedron (three contact points per primary sphere). The introduction of the agglomerates in the channel gives rise to three additional dimensionless numbers: an aspect ratio $\frac{a}{H}$, a solid-over-liquid density ratio $\frac{\rho_s}{\rho}$, and a solids volume fraction ϕ. The density ratio is relevant with a view to inertial effects, e.g. related to slip velocities, particle-particle and particle-wall collisions. We do not consider gravity in the simulations; it is assumed that $\frac{(\rho_s - \rho)g}{f_0} \ll 1$.

In this paper only part of the parameter space as identified above has been explored; Re_w, $\frac{a}{H}$, and $\frac{\rho_s}{\rho}$ have been fixed to values 2.6, 0.05 and 2.5 respectively (this density ratio is e.g. representative of glass beads in a watery liquid). We consider three solids volume fractions: ϕ=0.031, 0.062, and 0.093; three different types of agglomerates: doublets, triplets, and quadruplets; and three different flow geometries: a uniform channel ($\frac{h}{H} = 0$, see Fig. 1), and two channels with contractions having $\frac{h}{H}$=0.2 and 0.3. In all contracted channels $\frac{w}{L} = 0.1$.

3 Simulation procedure

In the simulations, a number of agglomerates made of equally-sized spheres (primary spheres) are placed in the liquid filled domain. The motion of the agglomerates and the liquid are fully coupled, i.e. the fluid flow sets the agglomerates in motion; the motion of the agglomerates on its turn induces fluid flow. The fluid flow we solve with the lattice-Boltzmann method (LBM). For flows in complexly shaped domains and/or with moving boundaries, this method has proven its usefulness [see e.g. the review article by Chen and Doolen (1998)]. In the LBM, the

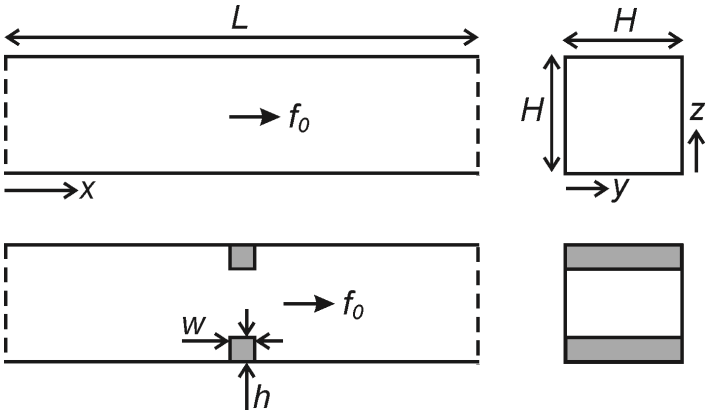

Figure 1: Definition of the flow channel and coordinate system. Top panels: uniform channel; bottom panels: channel with contraction. In the streamwise (x) direction periodic conditions apply.

computational domain is discretized into a number of lattice nodes residing on a uniform, cubic grid. Fluid parcels move from each node to its neighbors according to prescribed rules. It can be proven by means of a Chapman-Enskog expansion that, with the proper grid topology and collision rules, this system obeys, in the low Mach number limit, the incompressible Navier-Stokes equations [Chen and Doolen (1998), Succi (2001)]. The specific implementation used in our simulations has been described by Somers (1993), which is a variant of the widely used Lattice BGK scheme to handle the collision integral [e.g., see Qian, d'Humieres, and Lallemand (1992)]. We use the scheme due to Somers, as it manifests a more stable behaviour at low viscosities when compared to LBGK. A lattice-Boltzmann fluid is a compressible fluid. In order to mimic incompressible flow, as is done in this paper, the Mach number must be sufficiently low. In the simulations presented here the local Mach number never exceeded 0.05.

The fluid flow and the motion of the agglomerates are coupled by demanding that at the surface of each primary sphere the fluid velocity matches the local velocity of the solid surface (that is the sum of the linear velocity $\mathbf{v}_a$ and $\boldsymbol{\omega}_a \times (\mathbf{r} - \mathbf{r}_a)$ with $\boldsymbol{\omega}_a$ being the angular velocity of the agglomerate the primary sphere is part of, $\mathbf{r}_a$ is the agglomerate's center of mass, and $\mathbf{r}$ a point on the primary sphere's surface); in the forcing scheme that is applied here this is accomplished by imposing additional forces on the fluid at the surface of the primary spheres (which are then distributed to the lattice nodes in the vicinity of the particle surface). The details of the implementation of the forcing scheme can be found elsewhere [e.g. Ten Cate,

Nieuwstad, Derksen, and Van den Akker (2002)].

3.1 Determining forces and torques in agglomerates

The collection of forces acting on the fluid at the surfaces of the primary spheres forming an agglomerate is used to determine the hydrodynamic force and torque acting on that agglomerate (action = -reaction). In addition to the hydrodynamic force and torque stemming from the LBM, the motion of the agglomerates is controlled by lubrication forces, and by forces arising from the soft-sphere interactions that we use to deal with collisions between agglomerates. The equations of (linear and rotational) motion that we solve for an agglomerate consisting of n primary spheres can be written as

$$\begin{aligned} nm_0 \frac{d\mathbf{v_a}}{dt} &= \sum_{i=1}^{n} \mathbf{F_i} \\ \frac{d\mathbf{L_a}}{dt} &= \sum_{i=1}^{n} (\mathbf{T_i} + \mathbf{F_i} \times (\mathbf{r_i} - \mathbf{r_a})) \\ \mathbf{L_a} &= \mathbf{I_a} \omega_\mathbf{a} \end{aligned} \tag{1}$$

with $\mathbf{v_a}$ and $\omega_\mathbf{a}$ the linear and angular velocity of the agglomerate, $m_0 = \rho_s \frac{4\pi}{3} a^3$ the mass of a primary sphere, and $\mathbf{I_a}$ the moment of inertia tensor of the agglomerate. The vector $\mathbf{r_i}$ is the location of the center of sphere i. The torque $\mathbf{T_i}$ on primary sphere i directly follows from the LBM / forcing scheme.

As already indicated above, the force on primary sphere i ($\mathbf{F_i}$ in Eq. 1) has – in principle – three contributions: the hydrodynamic force stemming from the LBM (and forcing scheme), a radial lubrication force, and a soft-sphere interaction force which is also radial. The latter two contributions are non-zero only if a primary sphere belonging to another agglomerate is in close proximity of sphere i. Since they are radial they do not contribute to the torque on the primary sphere.

The lubrication force is added as a hydrodynamic force in situations where two primary spheres belonging to different agglomerates are in close proximity and move relative to one another. At some stage of proximity - typically when the surfaces of the two spheres involved are less than one grid spacing apart - the (fixed, i.e. non-adaptive) grid cannot accurately resolve the hydrodynamic interactions anymore and radial lubrication is explicitly added [Nguyen and Ladd (2002)]. A soft-sphere approach has been used to deal with collisions between primary spheres belonging to different agglomerates. In this approach a linear elastic repulsive force is switched on when spheres are in close proximity. It effectively prevents particles from overlapping and gives rise to fully elastic collisions.

The simulations provide us with the force and torque on each of the primary spheres ($\mathbf{F_i}$ and $\mathbf{T_i}$). From solving the set of Eq's 1 we know the acceleration (linear and rotational) of the agglomerate as a whole so that we also know the acceleration of each primary sphere:

$$\begin{aligned} \frac{d\mathbf{v_i}}{dt} &= \frac{d\mathbf{v_a}}{dt} + \frac{d}{dt}\left(\boldsymbol{\omega}_\mathbf{a} \times (\mathbf{r_i} - \mathbf{r_a})\right) \\ \frac{d\boldsymbol{\omega}_\mathbf{i}}{dt} &= \frac{d\boldsymbol{\omega}_\mathbf{a}}{dt} \end{aligned} \tag{2}$$

As a consequence we can determine the force $\mathbf{F_{c,i}}$ and torque $\mathbf{T_{c,i}}$ required to keep each primary sphere attached to the agglomerate:

$$\begin{aligned} \mathbf{F_{c,i}} &= m_0 \frac{d\mathbf{v_i}}{dt} - \mathbf{F_i} \\ \mathbf{T_{c,i}} &= I_0 \frac{d\boldsymbol{\omega}_\mathbf{a}}{dt} - \mathbf{T_i} \end{aligned} \tag{3}$$

(with $I_0 = \frac{2}{5}a^2 m_0$ the moment of inertia of the primary sphere about its center).

If primary sphere i has more than one contact point with other primary spheres in the agglomerate, $\mathbf{F_{c,i}}$ and $\mathbf{T_{c,i}}$ are the sum of contact forces and torques respectively. In the general case of an agglomerate arbitrarily configured of equally sized, contacting spheres it is not possible to determine the force and torque per contact point based on the collection of $\mathbf{F_{c,i}}$'s and $\mathbf{T_{c,i}}$'s only: Solving for forces and torques per contact point poses an ill defined problem. Additional physics e.g. related to mutual particle displacement within the agglomerate under mechanical loading is required to close the system of equations. Still, we consider the availability of the summed contact forces and torques per primary sphere to be useful information for assessing breakage probability.

However, in this paper we will be considering three simple agglomerates for which the forces and torques per contact point can be determined directly based on $\mathbf{F_{c,i}}$ and $\mathbf{T_{c,i}}$ (i=1...n): doublets, triplets, and quadruplets. The doublet has a single contact point and the resulting $\mathbf{F_{c,i}}$ and $\mathbf{T_{c,i}}$ are the force and torque in that single contact. The triplets are arranged in a triangle with two contact points per primary sphere; the quadruplets are arranged in a tetrahedron with three contact points per primary sphere. By making a few sensible assumptions the force (and torque) per contact point can be determined based on the set of $\mathbf{F_{c,i}}$ and $\mathbf{T_{c,i}}$ per primary sphere.

In an earlier paper [Derksen (2008)] we have applied the computational procedure as outlined above to study (among other things) flow-induced forces in sphere doublets undergoing simple shear flow. In that paper grid effects were assessed by varying the spatial resolution between 6 and 12 lattice spacings per primary sphere

radius a. The variation in resolution had hardly any effect (less than 2%) on the flow-induced force between the spheres. In the present study all simulations had a resolution such that $a = 6$.

4 Results

4.1 Flow field impressions

Although the flow in the channel is laminar, the presence of the agglomerates adds fluctuations and small-scale structures to the overall flow. We see that if we plot instantaneous realization of the flow in terms of contours of the velocity magnitude, and (clearer) in terms of the generalized deformation rate $\dot{\gamma} = \sqrt{2d_{ij}d_{ij}}$ (with $d_{ij} = \frac{1}{2}\left(\frac{\partial u_j}{\partial x_i} + \frac{\partial u_i}{\partial x_j}\right)$ the deformation rate tensor) as is done in Fig. 2. It is also important to see that the agglomerates do not experience a homogeneous deformation rate around them so that estimating flow-induced disruptive forces based on the deformation rate of the undisturbed flow (the flow without agglomerates) is a coarse approximation at best.

Obviously, with the same body force acting on the liquid, the flow rates in the channels reduce if a contraction is present; see Fig. 3. Therefore, compared to uniform channel flows at the same Reynolds number (and thus the same body force) contracted channel flows not necessarily have higher overall (i.e. volume averaged) deformation rates. Deformation tends to increase locally as a result of the more complicated flow structure in a contracted channel, and tends to decrease as a result of decreased flow rate and quiescent parts of the flow away from the contraction. Cleary the contractions have strong impact on the spatial distribution of liquid deformation over the channel; compare the deformation fields of Fig. 3 with the deformation field in Fig. 2. We expect this to have impact on the forces experienced at the contact points of the primary spheres in the agglomerates.

4.2 Flow and collision-induced forces in agglomerates

During the simulations we keep track of the entire force and torque history of every agglomerate so that we can reconstruct the contact forces and torques as a function of time. The discussion of the results in this paper focuses on the normal contact force. This is the projection of the contact force on the line connecting the centers of the two spheres sharing the contact point under consideration. A tensile normal contact force is positive; a compressive normal contact force is negative. Note that the simulations provide us with the full (three-dimensional) contact force vectors and contact torque vectors for every contact point in every agglomerate at every moment in time. Which components and/or projections of forces and torques are critical for agglomerate breakage depends on the physics and/or chemistry of the

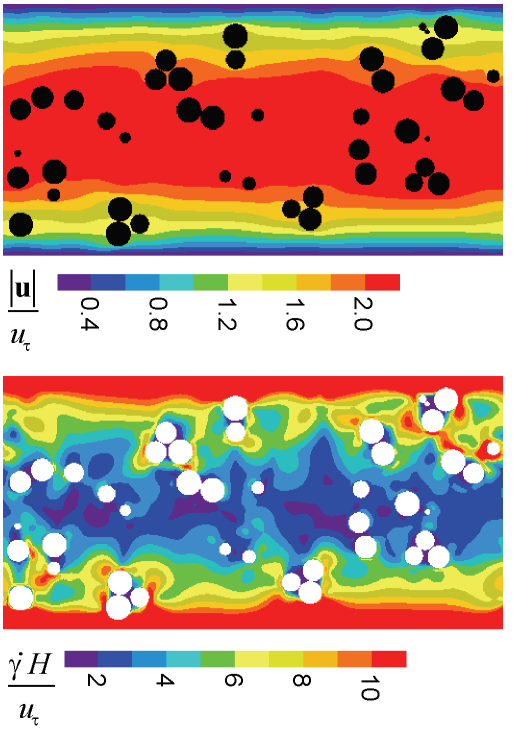

Figure 2: Contours of velocity magnitude (top) and deformation rate $\dot{\gamma}$ in the center plane of the uniform channel. The circular disks represent the cross sections of the spherical particles in the same center plane. Quadruplets, ϕ=0.093.

bonds between the primary spheres forming the agglomerates. This is a subject beyond the scope of the present paper. The discussions regarding the normal contact force allow us to show the detailed level of information gathered by the simulations, and to indicate some major trends in parameter space while not overloading the reader with the full (vectorial) contact force and torque information.

In Fig. 4 we show samples of time series of the normal force. It has been non-dimensionalized according to $F_n^* = \frac{F_n}{\mu \dot{\gamma}_w a^2}$, with $\dot{\gamma}_w = \frac{\tau_w}{\mu}$, with dimensionless time being $t^* = t\dot{\gamma}_w$. Each time series corresponds to one contact point in one agglomerate. The top panel compares simulations with quadruplets at three solids volume fractions, the middle panel compares three channel layouts (again for quadruplets), and the bottom panel compares doublets, triplets and quadruplets.

The smooth parts of the time series relate to the agglomerate translating and rotating through the laminar flow with a continuous change in the direct laminar hydrody-

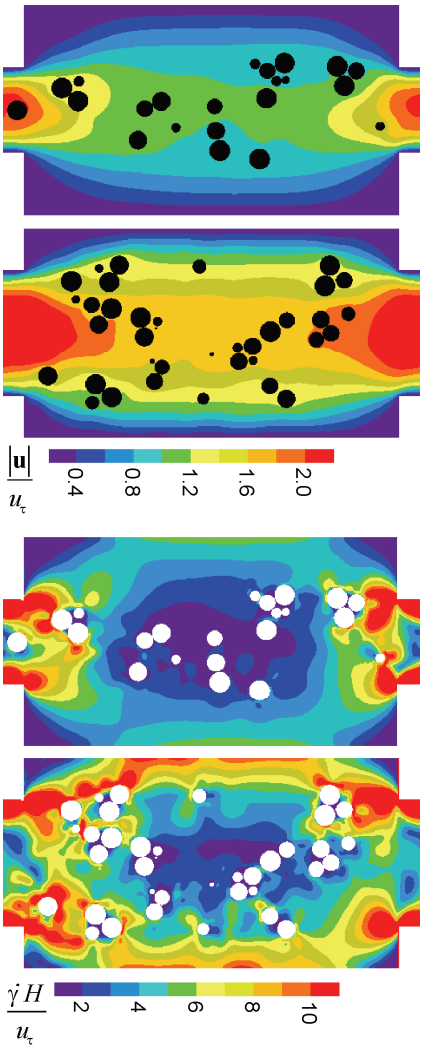

Figure 3: Contours of velocity magnitude (top two panels) and deformation rate $\dot{\gamma}$ for quadruplets in channels with contractions $\frac{h}{H}$=0.3 and 0.2 respectively. ϕ=0.062.

namic environment resulting in a gradual change in the normal force. The time scale of these smooth fluctuations is of the order of $\frac{10}{\dot{\gamma}_w}$. The spikes and apparent discontinuities in the force signal are due to collisions with other agglomerates in the channel.

Comparing the different time series obtained under different conditions and in dif-

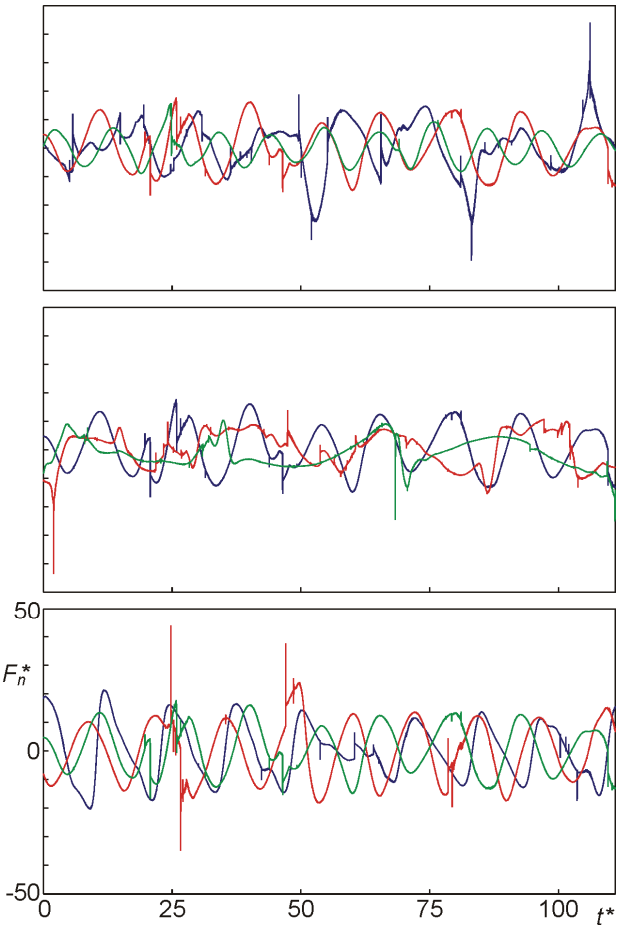

Figure 4: Time series of the normal force in a single point of contact. Force has been normalized according to $F_n^* = \frac{F_n}{\mu \dot{\gamma}_w a^2}$, time according to $t^* = t\dot{\gamma}_w$ with $\dot{\gamma}_w = \frac{\tau_w}{\mu}$ the average wall shear rate. Top panel: quadruplets in a uniform channel with solids volume fraction ϕ=0.093 (blue curve), 0.062 (red), 0.031 (green). Middle panel: quadruplets at ϕ=0.062 in a uniform channel (blue), a channel with contraction $\frac{h}{H}$=0.2 (red), a channel with contraction $\frac{h}{H}$=0.3 (green). Bottom panel: doublets (blue), triplets (red), quadruplets (green) in a uniform channel at ϕ=0.062.

ferent channels hints at a few trends. In the denser suspension the agglomerate collides more frequently leading to a normal-force signal with more spikes (top panel of Fig. 4). Also the flow seen by the agglomerate is more complex in the denser suspension. This leads to the smooth fluctuations of the signal in the denser

suspension having higher amplitude and higher frequencies. The effect of the contraction appears to be a reduction in the amplitude of the normal force (middle panel of Fig. 4). The agglomerates passing through the contraction can be reconstructed from these time series. A low-frequency variation of the force signal is from time to time followed by faster fluctuations when the agglomerate passes through the contraction. Comparing the force time series in doublets, triplets, and quadruplets does not indicate a clear trend. For this specific time series, triplets show somewhat stronger force fluctuations than doublets and quadruplets.

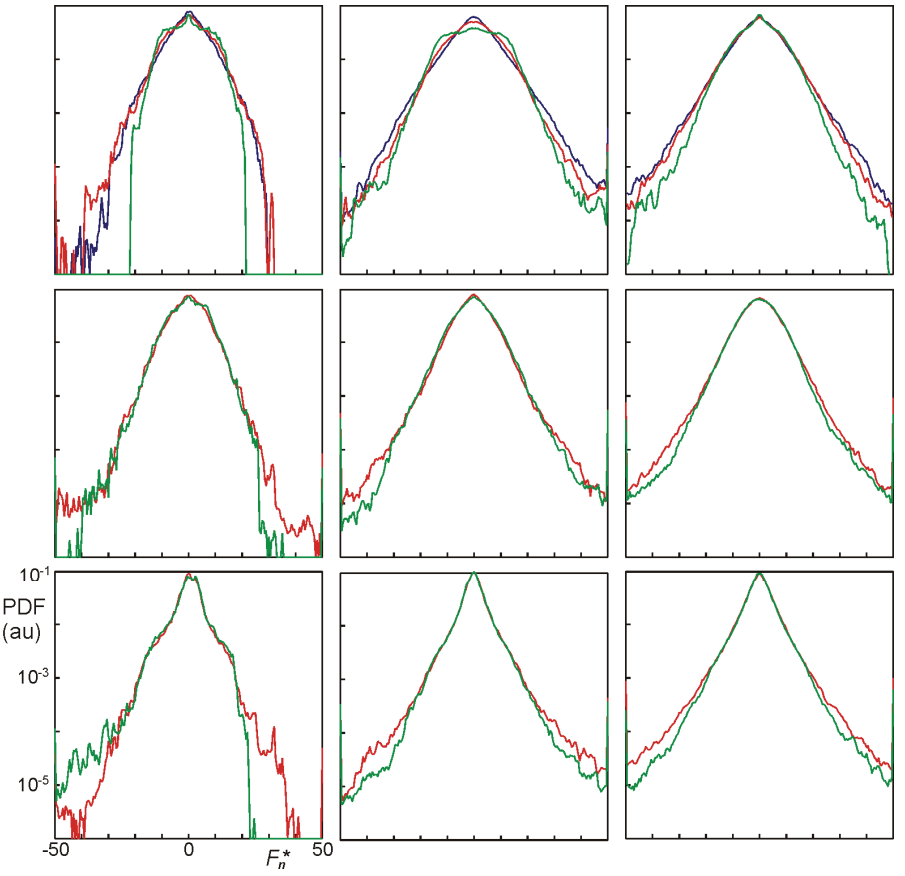

Figure 5: Probability density functions (PDF's) of the normal contact force. From left to right: doublets, triplets, and quadruplets. From top to bottom: uniform channel, contracted channel with $\frac{h}{H}$=0.2, and contracted channel with $\frac{h}{H}$=0.3. Blue curves have ϕ=0.093, red curves have ϕ=0.062, green curves have ϕ=0.031.

In order to more quantitatively analyze the normal force data based on the full amount of information contained in the simulations we condensed the normal forces in all contact points in all agglomerates at each moment in time in force probability density functions (PDF's), and organized them in Fig. 5. A number of interesting dependencies can be observed in the various panels of Fig. 5, and by comparing the various panels presented there. An apparent trend relates to the solids volume fraction. The more agglomerates, the higher the chances for collisions and thus the higher the chances for high normal force levels. As a results, the tails (high and low-end) of the PDF's for the higher solids volume fractions lie systematically above those for the lower solids volume fractions. The exception is the lower left panel of Fig. 5 (doublets in a strongly contracted channel) where the compressive forces in the ϕ=0.031 slurry are higher than those in the ϕ=0.062 agglomerate slurry.

The force PDF's of the different agglomerate types (doublets, triplets, quadruplets) in the uniform (i.e. non-contracted) channels (top row of Fig. 5) differ significantly. The (smaller) doublets have narrower PDF's than the triplets and quadruplets. The difference not only relates to size but also to shape. The doublets (at least the ones in the center portion of the channel) tend to align with the flow, specifically if the solids volume fraction is low so that collisions do not scatter the orientations. These effects reduce the chance of collisions and also reduce the (absolute value of) the contact force since the spheres in the aligned doublet see more or less the same hydrodynamic environment. There are minor differences between the force distributions of triplets and quadruplets.

Changing the channel geometry by placing contractions influences the flow-induced forces. For the quadruplets and the triplets the trend is from more Gaussian-shaped distributions (quadratic on the lin-log-scale of Fig. 5) for uniform channels towards exponential distributions (linear on lin-log-scale) for the strongest contractions. For the doublets the trends as a result of contractions are less systematic; we do observe a widening of the normal force PDF as a result of placing a contraction.

Dimensionless force peak levels $F_n^* = \frac{F_n}{\mu \dot{\gamma}_w a^2}$ are of the order of 50 (see Fig. 5). The wall shear rate $\dot{\gamma}_w = \frac{\tau_w}{\mu}$ is at the high end of the shear rates that would be present in the undisturbed (single phase) laminar flow. Based on undisturbed channel flow with $\dot{\gamma}_w$ we would estimate normal forces as high as $F_n^* \approx 20$[e.g. see Nir and Acrivos (1973)]. The complexity of the direct (hydrodynamic) environment of the agglomerates and collisions thus significantly add to the normal force peak-levels.

5 Conclusions

Motivated by the potential role of liquid deformation in the breakage of agglomerates we have set up a computational procedure for determining flow-induced forces in agglomerates and applied it for three simple agglomerate configurations (doublets, triplets and quadruplets all made of equally sized spheres) in laminar channel flow. The simulations fully resolve the liquid flow which is two-way coupled with the motion of the agglomerates. The flow simulations are based on lattice-Boltzmann discretization; collisions between agglomerates are based on a soft-sphere approach. During the simulations, the agglomerates keep their integrity and we keep track of the forces at the contact points required to keep the spheres the agglomerates are made of attached.

In terms of probability density functions (PDF's), the forces in the agglomerates depend on the solids volume fraction in the agglomerate slurry with increased chances for high force levels at high solids loading. This is largely due to collisions probabilities increasing in denser suspensions, but also due to the more complex hydrodynamic environment of an agglomerate in a dense suspension. Sphere doublets experience weaker normal forces compared to triplets and quadruplets.

We also investigated the impact of a contraction placed in the channel on the flow-induced force levels. Sharp contractions have been used in experiments to promote agglomerate breakage [Zaccone, Soos, Lattuada, Wu, Bäbler, and Morbidelli (2009)]. In our study contracted channels have been compared with uniform channels on the basis of equal pressure drop. This implies that the volumetric flow rate in the contracted channel is smaller than in uniform channel. Still (in general) the contracted channels widen the normal force PDF's hinting at their usefulness for promoting breakage.

Future work will be in applying the procedures for determining flow-induced forces in agglomerates to more generic flows, first and foremost homogeneous, isotropic turbulence. Such simulations will allow us to relate turbulence characteristics such as energy dissipation rate and Kolmogorov scale (relative to agglomerate size) with force and torque levels in agglomerates. This information would be useful for assessing breakage probabilities in turbulent, large-scale process equipment flows. Performing simulations with finite-strength agglomerates is another direction for future work. In such simulations we actually would break agglomerates if certain threshold forces, torques, and/or stresses are exceeded. By specifying direct interparticle force fields we could even study the interplay between agglomerate morphology and fluid flow.

Acknowledgement: Support of the Schlumberger DBR Technology Center is

gratefully acknowledged.

References

Aamir, E.; Nagy, Z.K.; Rielly, C.D.; Kleinert, T.; Judat, B. (2009): Combined quadrature method of moments and method of characteristics approach for efficient solution of population balance models for dynamic modeling and crystal size distribution control of crystallization processes. *Ind. & Engng. Chem. Res.*, vol. 48, pp. 8575-8484.

Bäbler M.U.; Morbidelli M.; Baldyga J. (2008): Modelling the breakup of solid aggregates in turbulent flows. *J. Fluid Mech.*, vol. 612, pp. 261-289.

Boek, E.S.; Ladva, H.K.; Crawshaw, J.P.; Padding, J.T. (2008): Deposition of Colloidal Asphaltene in Capillary Flow: Experiments and Mesoscopic Simulation. *Energy & Fuels*, vol. 22, pp. 805-813.

Chen, S.; Doolen, G.D. (1998): Lattice Boltzmann method for fluid flows. *Annual Rev. Fluid Mech.*, vol. 30, pp. 329-364.

Derksen, J.J. (2008): Flow induced forces in sphere doublets. *J. Fluid Mech*., vol. 608, pp. 337-356.

Hounslow, M.J.; Reynolds, G.K. (2006): Product engineering for crystal size distribution. *AIChE J*., vol. 52, pp. 2507-2517.

Nir, A.; Acrivos, A. (1973): On the creeping motion of two arbitrary-sized touching spheres in a linear shear field. *J. Fluid Mech*., vol. 59, pp. 209-223.

Nguyen, N.-Q.; Ladd, A.J.C. (2002): Lubrication corrections for lattice-Boltzmann simulations of particle suspensions. *Phys. Rev. E*, vol. 66, paper 046708.

Qian, Y.H.; d'Humieres, D.; Lallemand, P. (1992): Lattice BGK for the Navier-Stokes equations. Europhys. Lett., vol. 17, pp. 479-484.

Somers, J.A. (1993) Direct simulation of fluid flow with cellular automata and the lattice-Boltzmann equation. *App. Sci. Res*., vol. 51, pp. 127-133.

Succi, S. (2001): *The lattice Boltzmann equation for fluid dynamics and beyond*. Clarendon Press.

Ten Cate, A.; Nieuwstad, C.H.; Derksen, J.J.; Van den Akker, H.E.A. (2002): PIV experiments and lattice-Boltzmann simulations on a single sphere settling under gravity. *Phys. Fluids*, vol. 14, pp. 4012-4025.

Zaccone A.; Soos M.; Lattuada M.; Wu H.; Bäbler M.U.; Morbidelli M. (2009): Breakup of dense colloidal aggregates under hydrodynamic stresses. *Phys. Rev. E*, vol. 79, paper 061401.